Attribute expression of basement faulting—Time versus depth migration

SUAT AKTEPE, University of Houston, USA
KURT J. MARFURT and RODERICK PEREZ, University of Oklahoma, Norman, USA

The usual focus of seismic exploration for hydrocarbons is to directly image structural, stratigraphic, and diagenetic features in the "soft" sedimentary sequence. However, understanding the geologic processes that gave rise to these shallow features often requires an understanding of the structural deformation of the more "rigid" basement. In the Fort Worth Basin of north Texas, the end product is usually prestack time-migrated sections which indicate that shallow faulting may be basement-controlled. However, there is some doubt as to whether the collapse features in the sedimentary section are controlled by what appear to be rhombochasms in the basement, or whether these rhombochasms are a velocity push-down artifact caused by infill of the collapse features by a slower velocity material. The goal of this study is to improve the image quality of such basement features by the use of more interpreter-driven detailed velocity analysis and depth versus time migration.

The key to accurate imaging is accurate velocity analysis. Rather than performing our velocity analysis on a regular grid, we use time slices through geometric attribute images computed from the original prestack time-migrated data volumes to avoid using inaccurate velocity estimates near faults and to add extra velocity analysis points within down-dropped blocks, thereby avoiding smoothing through them and perhaps inducing velocity push-down artifacts. We find that the time- and depth-migration images are comparable at the target shale horizon. However, the depth-migration basement images are significantly different, with a strong domal basement feature underlying the survey, better-delineated basement faulting, and discrete down-dropped blocks clearly defined in the prestack depth migration images.

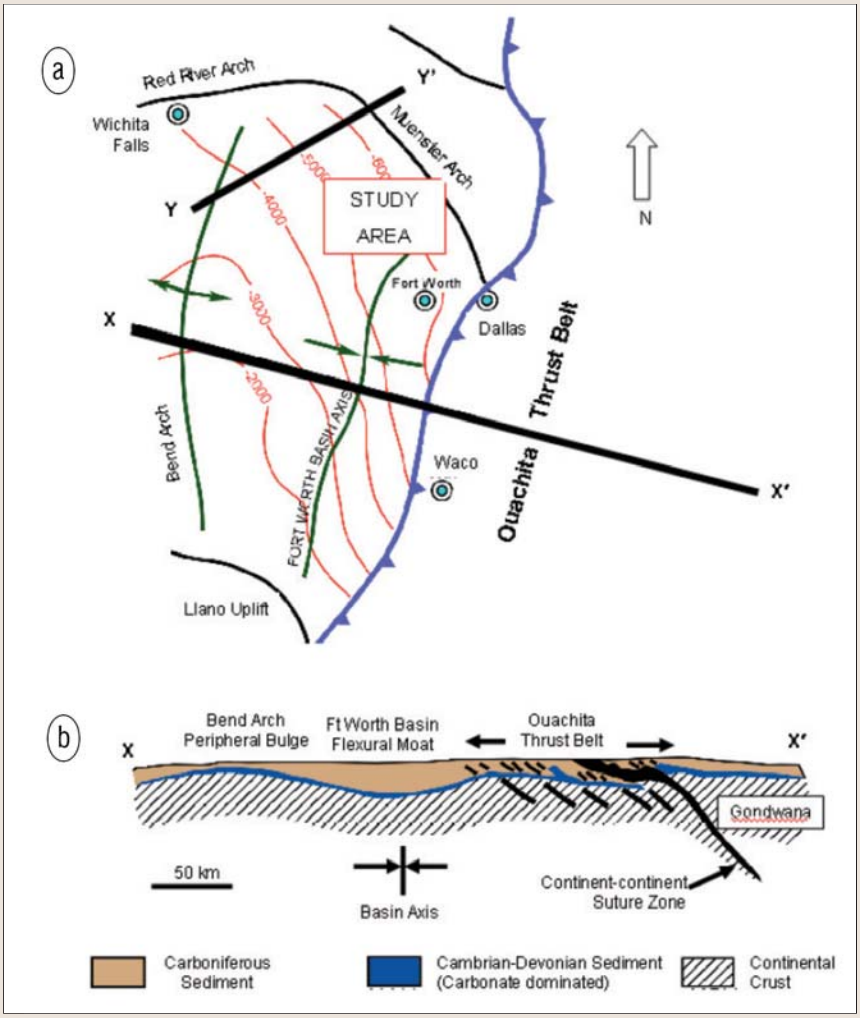

Figure 1. *Map view and cross-section through the Fort Worth Basin and Ouachita thrust belt. The basin developed as a foredeep and underwent compression and strike-slip deformation during the Pennsylvanian, followed by Mesozoic and Cenozoic extension. Collapse breccias compartmentalize Pennsylvanian reservoirs in the study area (after Hardage et al., 1996).*

Motivation. While the objective of each processing step is to improve our seismic image of the subsurface, algorithms that are either "more sophisticated" or more computationally intensive do not always improve our results. While the shallow structures in the Fort Worth Basin, including the Barnett shale, are adequately illuminated by prestack time migration, the sediments and basement underlying the Cambro-Ordovician Ellenburger limestone are not. 3D volumetric attributes are easy to compute and able to delineate features of geologic interest, particularly on uninterpreted time and depth slices. For this reason, we evaluate the value of each processing step by measuring the impact on interpretation. We apply this workflow to poststack and prestack time- and depth-migration results from Fort Worth Basin data with the specific goal of delineating faults and folds in the basement. Fracture, kinematic, and burial histories are the keys to understanding the deformation process in the basin during geologic time. Any element that helps to enhance this knowledge is important.

Geologic setting. The Fort Worth Basin (FWB) is a shallow foreland basin, north–south elongated, encompassing roughly 15 000 mi^2 (39 000 km^2), located in north Texas. The tectonic and structural history of the FWB is very complex and involves several episodes. The first episode is the collision between North and South America, resulting with the closure of the Iapetus Ocean (Lahti and Huber, 1982; Walper, 1982) during the Mississippian to the Early Permian. In this step, the basin was downwarped in response to the tectonic

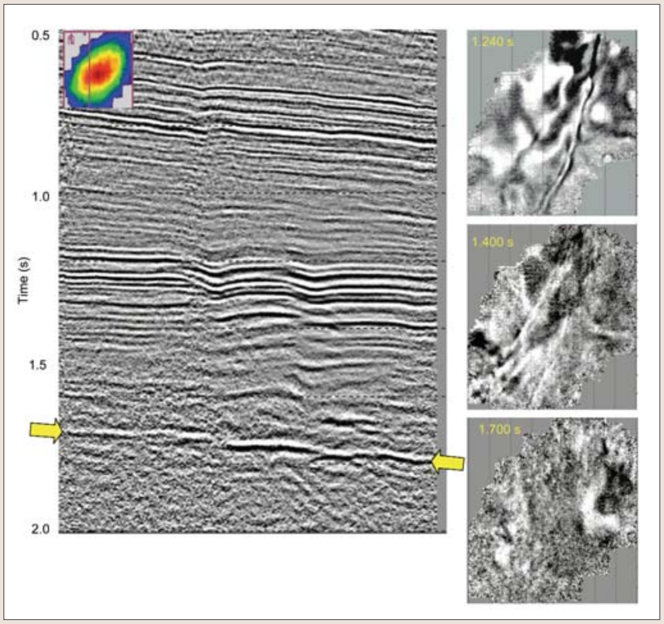

Figure 2. Stacked data along a representative inline AA′ whose location is shown in the fold map inserted in the upper left. Arrows indicate interpreted basement. On the right are time slices through the stacked volume at 1.240 (approximate Mississippian shale), 1.400 (approximate Ordovician carbonate), and 1.700 s (approximate basement). The goal is to accurately image stratigraphic features and subtle faults and karst in the Mississippian shale. Nevertheless, note the decrease in data quality at deeper levels.

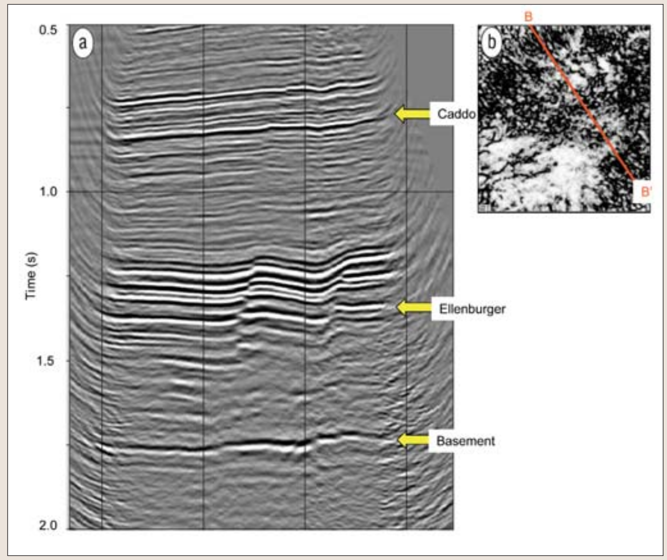

Figure 3. Poststack time-migrated (a) vertical section through the seismic amplitude along line BB′ and (b) time slice at 1.7 s at the approximate basement level through the corresponding coherence volume. Yellow arrows indicate the top of the Pennsylvanian Caddo, Cambro-Ordovician Ellenburger, and basement horizons. The basement is well-illuminated and faults appear to align.

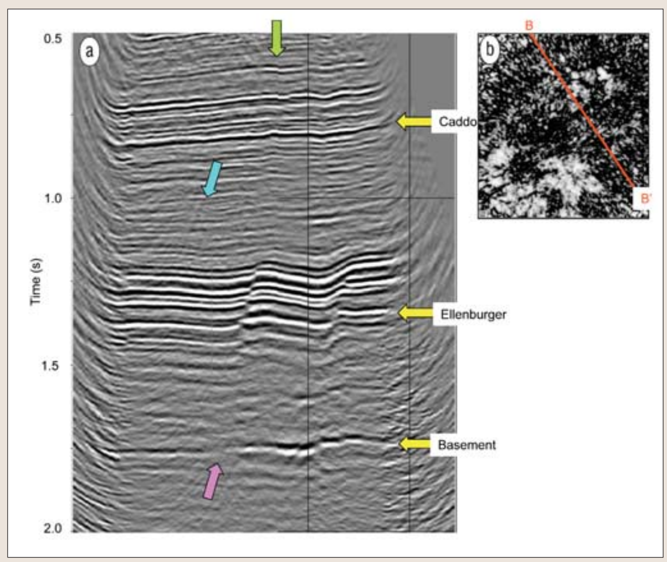

Figure 4. Prestack time-migrated (a) vertical section through the seismic amplitude along line BB′ and (b) time slice at 1.7 s at the approximate basement level through the corresponding coherence volume. Yellow arrows indicate the top of the Pennsylvanian Caddo, Cambro-Ordovician Ellenburger, and basement horizons. Shallow faults such as that indicated by the green arrow are better delineated. There is a slight increase in lateral resolution above the Ellenburger. However, migration artifacts (cyan arrow) contaminate the image, while the basement is less well illuminated in the zone indicated by the magenta arrow.

stresses that formed the Ouachita thrust belt in the early Pennsylvanian (Johnson et al., 1988). The maximum thickness in the FWB appears close to the Muenster arch, and approaches 12 000 ft (3700 m).

The Ouachita trust belt was formed during the Pennsylvanian (Thompson, 1988), as a result of the collision of North and South America during the Paleozoic, followed by Mesozoic and Cenozoic extension (Walper, 1982). Figure 1 summarizes the main structural features in the basin. Currently, this basin is a major object of interest because of the presence of high TOC Mississippian shale sediments, which are a target for exploration and development of unconventional shale gas resources.

Limited core information indicates that the FWB basement consists of Precambrian granodiorites and metasediments, overlain by 3000 ft (900 m) of a Cambrian section comprising the Willberns, Riley, and Hickory formations and an Ordovician carbonate section formed by the Ellenburger–Simpson Groups and the Viola limestone (Montgomery, 2005). The Viola Formation was subjected to an extensive and severe period of exposure resulting from a dramatic drop in the sea level during the Ordovician related with the regional uplift of the basin (Henry, 1982). This drop in the sea level resulted in the exposure of the carbonate platform forming karst features and erosion of an undefined part of the sequence (Kerans, 1988). The mostly dolomitic Ellenburger Group exhibits high porosity resulting from the development of karst features, and is often a water-bearing formation that can destroy shallower gas production in the shale reservoir through connectivity of either natural or induced fractures. In the area of study, the Mississippian Barnett Shale was deposited directly over the eroded Viola limestone strata, on a shelf or in a basin area marginal to the Ouachita geosyncline. The Barnett shale sequence consists of alternating shallow marine limestones and black, organic rich shales. In the eastern side of the FWB, the Barnett shale can be subdivided into an upper- and a lower-interval unit interbedded by a dark limestone interval, known as the Forestburg limestone. The Forestburg is absent in the south and west of this survey and is not an exploration target. However, it forms an effective fracture barrier to contain the induced hydraulic fractures in the gas wells. The presence of glauconite and phosphate material indicates slow deposition under reducing conditions. The FWB acted as an ideal depocenter to sediments from the Ouachita thrust belt and the Muenster arch, (Walper, 1982;

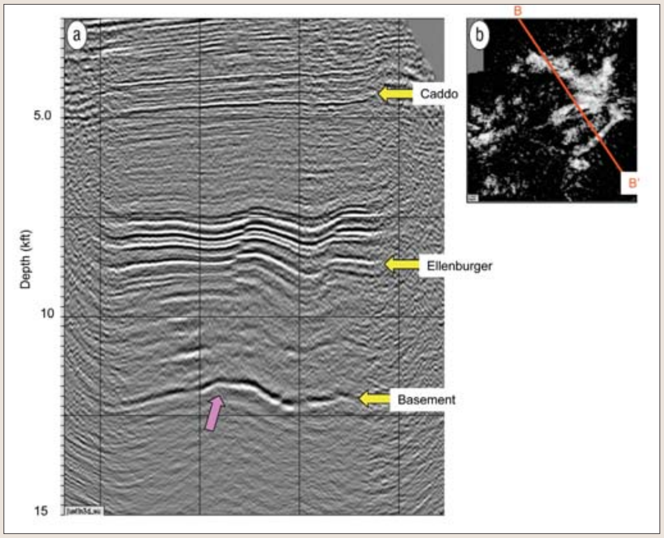

Figure 5. Poststack depth-migrated (a) vertical section through the seismic amplitude along line BB′ and (b) time slice at 12 000 ft at the approximate basement level through the corresponding coherence volume. Yellow arrows indicate the top of the Pennsylvanian Caddo, Cambro-Ordovician Ellenburger, and basement. While the image is contaminated by random migration noise, notice that we now observe a structural high in the basement (magenta arrow) that was not apparent in the either of the time-migrated images.

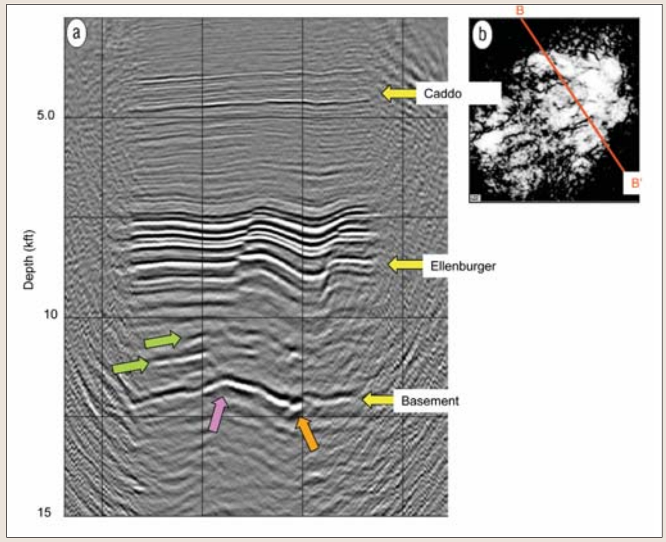

Figure 6. Prestack depth-migrated (a) vertical section through the seismic amplitude along line BB′ and (b) time slice at 12 000 ft at the approximate basement level through the corresponding coherence volume. Yellow arrows indicate the top of the Pennsylvanian Caddo, Cambro-Ordovician Ellenburger, and basement horizons. The basement high indicated by the magenta arrow is somewhat higher and more steeply inclined to the SE than in the poststack depth migration image. The down-dropped fault block indicated by the orange arrow in now rotated. Green arrows indicate reflectors in the Cambro-Ordovician section that were previously poorly illuminated.

Thompson, 1988). Subsequent siliciclastic sections including the Atoka and Caddo succeeded the deposition of the Marble Falls Limestone in the early Pennsylvanian.

Acquisition and processing. Devon Energy (and its predecessor, Mitchell Energy) is the first operator to exploit the Barnett shale. During the past decade, it has perfected its seismic acquisition programs to suppress ground roll and acquisition footprint, to maintain sufficiently high fold and azimuthal coverage to facilitate accurate azimuthal anisotropy analysis, and to provide high-resolution images. To our knowledge, all operators in the FWB have been satisfied with prestack time migration, typically followed by some form of high-frequency enhancement to enhance the thin formations of interest. The 3D survey treated here is the same one subjected to long-offset enhancement, data morphing, and a new azimuthal-binning approach presented by Perez and Marfurt (2007; 2008).

We obtained a copy of the Fort Worth data from the service company as unmuted, properly-indexed shot gathers. We performed a simple flow consisting of trace editing to suppress noise bursts, followed by deconvolution and bandpass filtering to attenuate ground roll and better balance the spectrum.

Velocity model. Prior to detailed velocity analysis, we used a single velocity function to migrate the entire survey which we used as our baseline processing flow. We used commercial software to pick velocity spectra, running three passes of velocity analysis. The first pass was on a coarse 50 × 50 CDP grid, the second pass on a finer grid of 20 × 20 CDPs, and the final pass on a 10 × 10 CDP grid. Additional velocity picks were made over suspected down-dropped blocks and collapse features that were not sufficiently analyzed by our fine grid in order to account for velocity push-down. Following the workflow described by Yilmaz (2001), we converted the picked stacking velocities to root mean square (rms) velocities. After some additional refinement, we converted the rms velocities to interval velocities.

By picking the horizons on the time-migrated volume and using the residual moveout updated rms velocity volume, we generated rms velocity maps along each interpreted horizon. The rms velocity maps were gridded along each picked horizon and converted to interval velocity maps, thereby generating a horizon-consistent interval velocity volume.

Time imaging. Most processors generate an NMO stack volume to both provide a preliminary imaging and to quality control statics and deconvolution parameters. Figure 2 shows a good image of the shallower horizons; however, the deeper horizons including the basement (indicated by yellow arrows) are somewhat smeared and contaminated by random noise.

We used the resulting stack and rms velocity volumes as input files to the poststack time migration process. First we conducted a process of systematic velocity model building, beginning with a coarse grid of velocity analysis.

During the second iteration in building our velocity model, we made our grid four times finer and then inserted irregularly located velocity analysis points where the initial images and geometric attributes (coherence and most negative curvature) indicated the existence of collapse features. Finally we applied 3D Kirchhoff time migration to the data set using our new velocity model that was relatively more sensitive to the collapse features. Figures 3 and 4 show vertical slices through the poststack and prestack time-migrated volumes along an arbitrary line BB′ perpendicular to the structural fabric.

Figures 3 and 4 are quite comparable with the poststack migrated image having less superposed migration artifacts (cyan arrow in Figure 4). Shallow faults such as that indicated by the green arrow in Figure 4 are better delineated on the prestack time-migrated data. There is also a slight increase in lateral resolution above the Ellenburger.

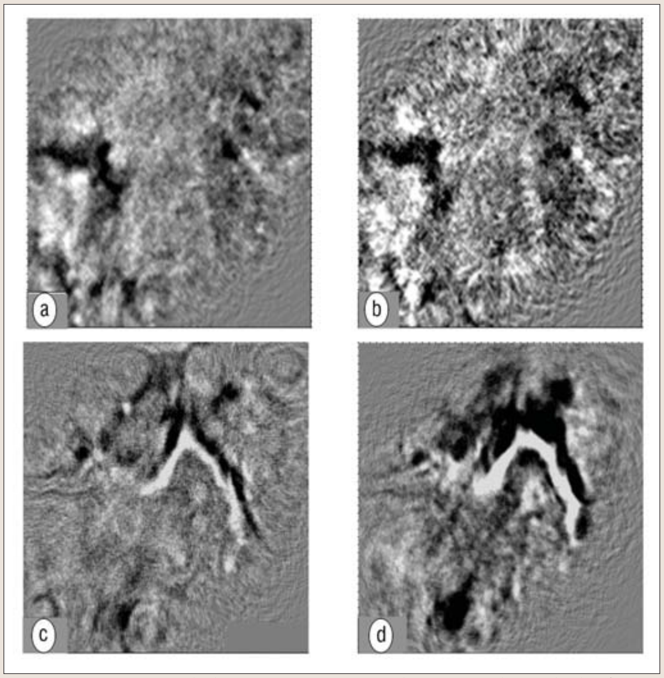

Figure 7. Horizontal slices at approximate basement through the four migrated seismic data volumes: (a) at 1.7 s through the poststack time-migrated data, (b) at 1.7 s through the prestack time-migrated data, (c) at 12 000 ft (3.6 km) through the poststack depth-migrated data, and (d) at 12 000 ft (3.6 km) through the prestack depth-migrated data. Note the improvement in clarity and signal-to-noise ratio in the prestack depth-migrated data. Also note that the amplitudes are stronger towards the edges for the two time-migrated data volumes.

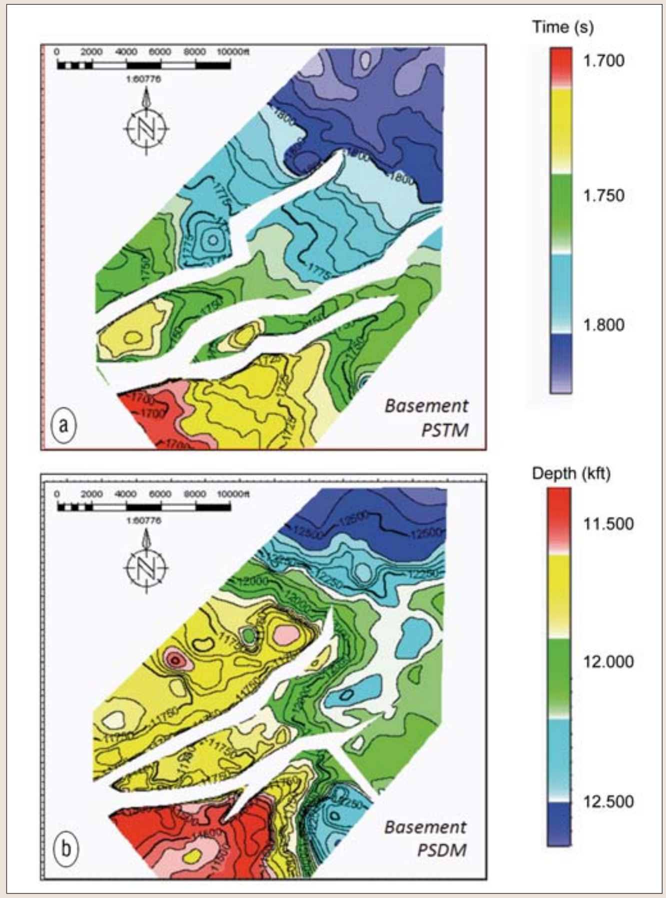

Figure 8. Time-structure maps of the basement interpreted from (a) prestack time-migrated, and (b) prestack depth-migrated volumes.

Depth imaging. We compute traveltime using a spherical eikonal traveltime algorithm and integrate the data over diffraction hyperbolae using the same 20 000 ft (6000 m) migration aperture that we used in pre- and poststack time migration. The CDP gathers were also subjected to 3D Kirchhoff prestack depth migration. The traveltime calculations and migration apertures were analogous to those used in poststack depth migration.

The poststack migration depth image is used as an initial model for the prestack depth-migration process. While the image Figure 5 is contaminated by random migration noise, notice that the basement now shows a structural high (magenta arrow) that was not apparent in the either of the time-migrated images. The impact of the thinner high-velocity Ellenburger carbonate formation overlying this structural high resulted in a velocity pull-up on its flanks, resulting in a relatively flat basement image in the time-migrated volumes shown in Figure 3 and 4.

Theoretically, if we have an accurate velocity model, prestack depth migration should be superior to poststack depth migration. We see that this is indeed the case in that we can now delineate a suite of coherent reflectors between the top of the Ellenburger and the basement that were previously buried in the noise (green arrows in Figure 6). The basement high indicated by the magenta arrow is somewhat higher and more steeply inclined to the SE than in the poststack depth migration image. The down-dropped fault block indicated by the orange arrow in now rotated.

Figure 7 shows horizontal slices at approximate basement at 1.7 s through the two time-migrated volumes and at 12 000 ft through the two depth-migrated volumes. Note the improvement in clarity and signal-to-noise ratio in the prestack depth-migrated data. Also note that the anticlinal basement structure is narrower on depth migration than on time migration.

Attributes. The coherence attribute is a powerful tool in imaging discontinuities such as fractures and faults on time, depth, and horizon slices. In Figures 3–6, we showed horizontal slices near the basement through coherence volumes computed from each of the migrated volumes. The prestack depth-migrated volume gives the best contrast between incoherent faults and coherent reflectors. We display basement maps picked from prestack time and depth-migrated volumes in Figure 8.

Next, we compare horizon slices along the basement through coherence, most-negative curvature, and most-positive curvature through the two time-migrated images in Figure 9. Although it may appear to be counter-intuitive, poststack time migration provides higher coherence images. Small faults and stratigraphic discontinuities are smeared and thus appear to be more coherent. The prestack time migration coherence has higher lateral resolution. Although the images in Figure 9 look very geological, we need to interpret them with great care. Comparison of Figures 3 and 4 with 5 and 6 shows that depth migration significantly changes the appearance of basement structure. In addition to geology, we need to think in terms of seismic processing artifacts. Under- and overmigrated discontinuities will be smeared and thus appear to be coherent. Crossing events perhaps associated with migration frowns and smiles appear as incoherent events and can be confused with geologic discontinuities. Some of the discontinuities seen in coherence in the time-migrated image are due to the well-known fault shadow effect. More gradual velocity-induced pull-up and push-down will directly impact our curvature images. The cyan arrow in Figure 10 indicates en-echelon faulting that is not easily seen on the other coherence images.

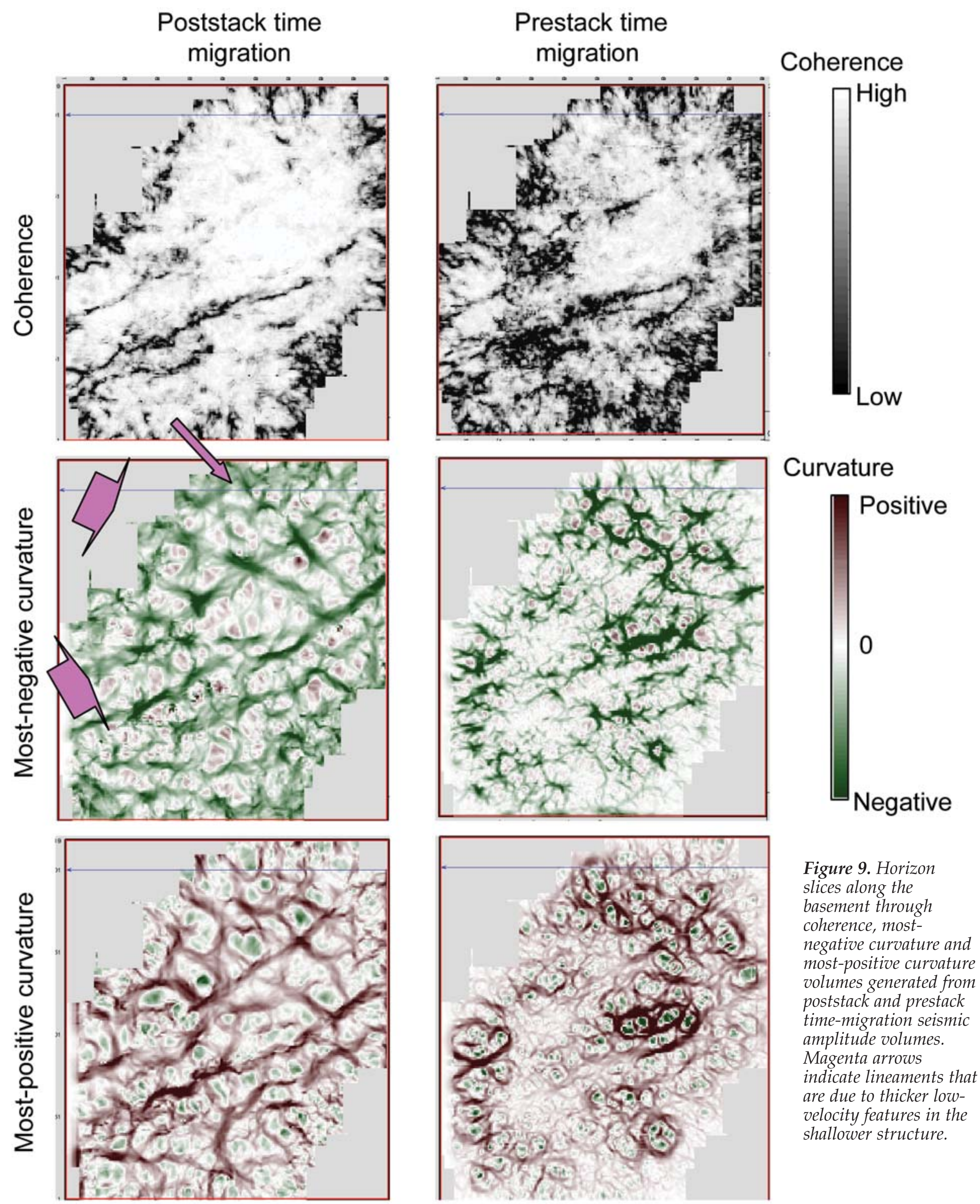

Figure 9. *Horizon slices along the basement through coherence, most-negative curvature and most-positive curvature volumes generated from poststack and prestack time-migration seismic amplitude volumes. Magenta arrows indicate lineaments that are due to thicker low-velocity features in the shallower structure.*

Most-negative curvature has been found to be particularly effective in carbonate terrains that have undergone diagenetic alteration, where karsts and faults appear as bowls and synclines. We interpret the lineaments indicated by the magenta arrows in Figure 9 to be an artifact associated with laterally variable velocity pull-up caused by faulting and thickening of the overlying fast Ellenburger Formation. Given our care in velocity analysis and the improved imaging of pre-Ellenburger reflectors, we interpret the "bowls" indicated by yellow arrows in the prestack depth-migrated most-positive curvature images shown in Figure 10 to be small collapse features seen in the basement.

Conclusions. In this study, we use a workflow consisting of velocity model building, imaging, and attribute calculation to image the basement in a survey acquired over the Fort Worth Basin, Texas. Our ultimate objective is to determine if suspected collapse features truly involve the basement, or if they are an

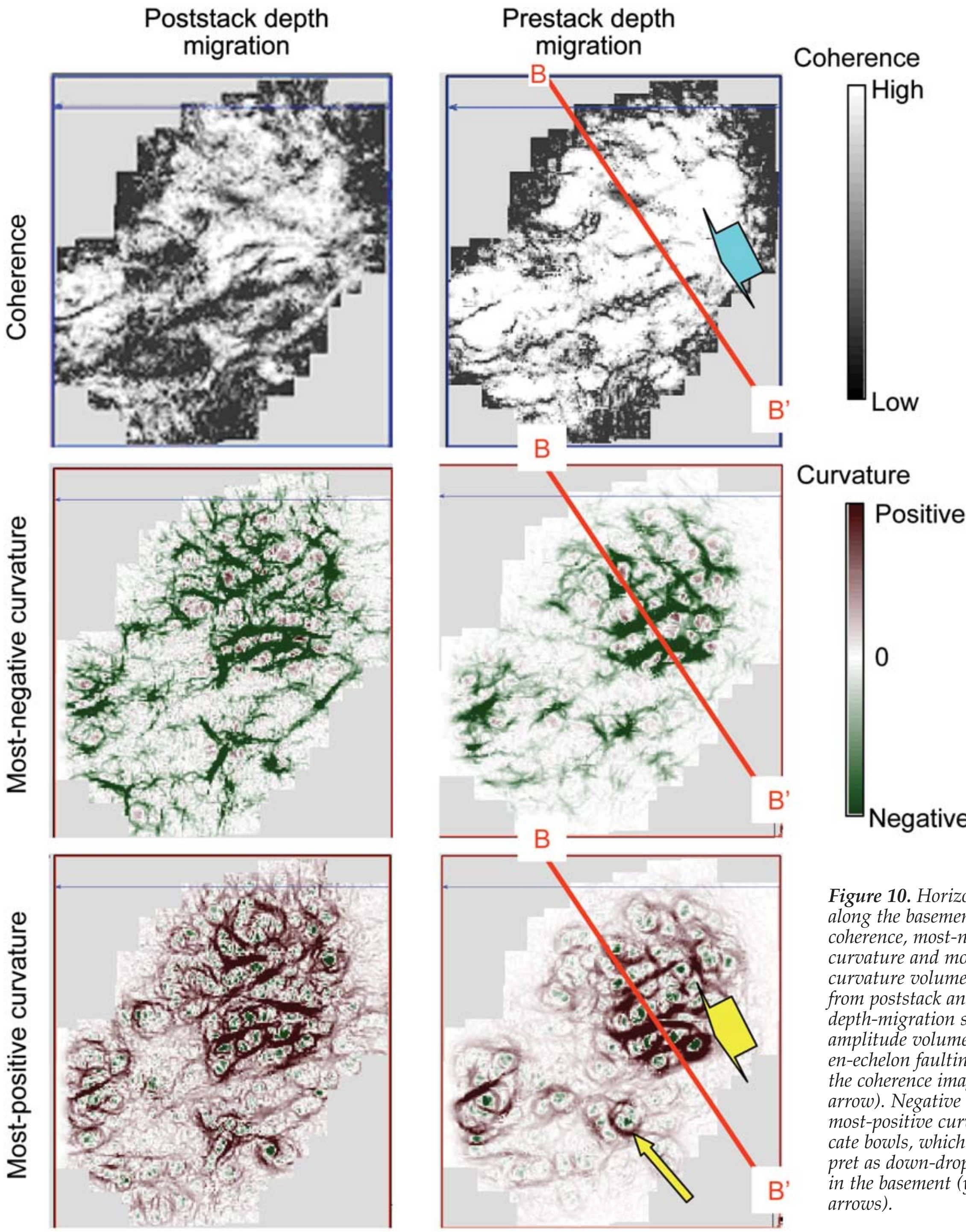

Figure 10. Horizon slices along the basement through coherence, most-negative curvature and most-positive curvature volumes generated from poststack and prestack depth-migration seismic amplitude volumes. Note the en-echelon faulting seen in the coherence image (cyan arrow). Negative values of most-positive curvature indicate bowls, which we interpret as down-dropped blocks in the basement (yellow arrows).

artifact due to velocity push-down of shallower karst features filled with low-velocity material.

Velocity model building is a crucial part of the subsurface imaging procedure. Since the target Barnett shale is adequately imaged through careful prestack time migration, few, if any, 3D surveys in this part of the world have been subjected to prestack depth migration. We find that prestack depth migration has a zero-order impact on our ability to accurately image the structure of reflectors below the high velocity Ellenburger Formation, including the basement. In general, velocity errors cause the misplacement of reflectors and a defocusing of the image. Specifically, incorrect velocities result in smeared fault images and a misalignment of reflector terminations with what otherwise might appear to be a smoothly varying fault surface. Coherence images of such faults will in general be less sharp than if properly imaged. In addition, inaccurate velocities and seismic imaging will result in migration smiles and frowns crossing reflectors of geologic interest. Such crossing events will appear to be low-coherence artifacts on time and horizon slices, confusing the interpretation of geologic features of interest.

Volumetric curvature has proven to be a particularly valuable tool in delineating subtle faults in the Fort Worth Basin. Reflector pull-up and push-down over laterally variable velocity fields will result in broad "processing artifacts" that are clearly delineated by applying most-positive and most-negative curvature to the deeper sections of our time-migrated data volumes. Prestack depth migration has several effects. First, it eliminates velocity pull-up and push-down. Second, it better focuses reflectors that were previously poorly focused—in our case, between the Ellenburger and the basement. Third, it delineates structural highs, lows, and faults that are truly in the geology.

The attribute images computed from the prestack depth-migrated images (Figure 10) suggest that there is significant faulting in the basement. The pattern of NE–SW and NW–SE faulting is consistent with that reported by Sullivan et al. (2006) in a different Fort Worth Basin survey lying 40 km to the west. Sullivan et al. interpret these faults and the collapse features between them as rhombochasms in a pull-apart basin. While not definitive without supporting well control, the images generated for this survey support a similar interpretation.

Suggested reading. "3D seismic evidence for the effects of carbonate karst breccia collapse on overlying clastic stratigraphy and reservoir compartmentalization" by Hardage et al. (GEOPHYSICS, 1996). "Stratigraphy of the Barnett Shale (Mississippian) and associated reefs in the northern Fort Worth Basin" by Henry (in *Petroleum Geology of the Fort Worth Basin and Bend Arch Area*, Dallas Geological Society, 1982). "Southern midcontinent region" by Johnson et al. (in *Sedimentary Cover—North American Craton, U.S.*, Geological Society of America, 1988). "Karst-controlled reservoir heterogeneity in Ellenburger Group carbonates of west Texas" by Kerans (*AAPG Bulletin*, 1988). "The Atoka Group (Pennsylvanian) of the Boonsville field area, north–central Texas" by Lahti and Huber (in *Petroleum Geology of the Fort Worth Basin and Bend Arch Area*, Dallas Geological Society, 1982). "Mississippian Barnett Shale, Fort Worth Basin, northcentral Texas: Gas-shale play with multitrillion cubic foot potential" by Montgomery et al. (*AAPG Bulletin*, 2005). "Improving lateral and vertical resolution of seismic images by correcting for wavelet stretch in common-angle migration" by Perez and Marfurt (GEOPHYSICS, 2007). "New azimuthal binning for improved delineation of faults and fractures" by Perez and Marfurt (accepted by GEOPHYSICS, 2008). "Warping prestack seismic data to improve stack quality and resolution" by Perez and Marfurt (accepted by GEOPHYSICS, 2008). "Application of new seismic attributes to collapse chimneys in the Fort Worth Basin" by Sullivan et al. (GEOPHYSICS, 2006). "Fort Worth Basin" by Thompson (in *Sedimentary Cover—North American Craton, U.S.*, Geological Society of America, 1988). "Plate tectonic evolution of the Fort Worth Basin" by Walper (in *Petroleum Geology of the Fort Worth Basin and Bend Arch Area*, Dallas Geological Society, 1982). *Seismic Data Processing* by Yilmaz (SEG, 2001). TLE

Acknowledgments: Suat Aktepe is currently with the Turkish Petroleum Corporation, Ankara, Turkey. The authors thank Devon Energy for permission to use and publish their data. Thanks to Joe Reilly of ExxonMobil for warning us of the possibility of velocity push-down on our basement structures. Suat Aktepe gives special thanks to Edip Baysal, Orhan Yilmäz, and Irfan Tanritanir for sharing their guidance, expertise, and encouragement during the study. Part of this study was supported by a DOE contract on "Improving geologic and engineering models of Midcontinent fracture and karst modified reservoirs using 3D seismic sttributes."

Corresponding author: kmarfurt@ou.edu